

Influences of Bubbles between Electrodes onto Efficiency of Alkaline Water Electrolysis

N. Nagai^{1*}, M. Takeuchi¹ and M. Nakao²

¹ Department of Mechanical Engineering, Fukui University, Japan
² Graduate School of Engineering, Fukui University, Japan

KEYWORDS:

Main subject(s): *Multi-Phase Flow, Micro Fluidic*

Fluid: *Hydrodynamics*

Visualization method(s): *Digital Microscope, Digital Video Camera*

Other keywords: *Water Electrolysis, Hydrogen Production*

ABSTRACT: There is an optimum condition on water electrolysis efficiency due to the effects of generated bubbles between electrodes. In this paper, in order to explain the existence of the optimum condition, a model of alkaline water electrolysis was established. The model can express void fraction and current density profiles along electrodes, and show the existence of the optimum condition. For verification of this model, rising velocity, diameter distribution of bubbles between electrodes and current density profiles along electrodes were measured during water electrolysis of KOH solution. Two-phase flows between electrodes were observed by digital microscope and digital video camera. The results showed that bubble rising velocity ranges from 4~25 cm/s and becomes larger as current density increases. Bubble diameter ranges from 0.01~0.5 mm, where average diameter becomes large as current density increases. Obtained results showed the sound validity of present model.

1. Introduction

Hydrogen energy is expected to be useful as secondary energy in the near future (Winter and Nitsch, 1988; Sandstede and Wurster, 1995), applicable to fuel for vehicle and rocket, chemical use, Ni-H₂ electric cell, thermal engine using hydrogen storage alloys, direct combustion for heat, and so on. In addition, hydrogen energy can be used to build up dispersive energy system together with electric power by combination of water electrolysis and fuel cell. In such an energy system, water electrolysis will become one of key technologies, and high performance of water electrolysis should be achieved.

The voltage needed to realize water electrolysis consists largely of reversible potential (=1.23V at 1 atm, 25°C), overvoltage on electrodes, and ohmic loss in aqueous solution (LeRoy et al., 1979). Reversible potential at a certain system temperature and concentration of aqueous solution can be determined electro-chemically by standard electrode potential and Nernst equation. Overvoltage on

* Corresponding author: Dr. Niro NAGAI, Department of Mechanical Engineering, Fukui University, 3-9-1 Bunkyo, Fukui 910-8507, Japan, Tel:+81-776-27-8537, Fax:+81-776-27-8748, email: nagai@mech.fukui-u.ac.jp

electrodes under smaller current density can be estimated basically by Butler-Volmer equation. For larger current density, overvoltage is dominated by diffusion of molecules and ions in solution. On purpose to realize higher efficiency of water electrolysis, many researches have been conducted so far, mainly focused on decrease of reversible potential and overvoltage on electrodes by realizing water electrolysis under high temperature and pressure or developing new electrode materials (Abe, et al., 1984). However, little attention has been paid to ohmic loss in aqueous solution from hydrodynamic and two-phase flow point of view.

LeRoy et al. (1979) pointed out that the increase of volume fraction of hydrogen or oxygen bubbles between electrodes, i.e. increase of void fraction, would cause the increase of electric resistance in aqueous solution, resulting in efficiency decrease of water electrolysis. The succeeding reports show analytical models of void fraction and current density profiles along electrodes, and experimental results of detailed information on void fraction, rising velocity and diameter distributions of bubbles (Funk et al., 1969; Hine and Sugimoto, 1980; Bongenaar et al., 1985; Janssen and Visser, 1991). Recently, Riegel et al. (1998) examined bubble diffusion, convection and transportation between electrodes in detail. These former works were successful to generally explain the effects of bubbles on water electrolysis efficiency at a rather low current density or a rather large electrode space. On the other hand, Nagai et al. (2003) found out that there is an optimum electrode space under high current densities. While the current density is small, the efficiency of water electrolysis becomes larger as electrodes space decreases, since the electric resistance between electrodes decreases. When the current density is rather high and the space is rather small, however, the void fraction between electrodes gets rather large resulting in increasing electric resistance between electrodes, and then decreasing the efficiency of water electrolysis.

In this report, therefore, a model on alkaline water electrolysis was established, incorporating the influences of generated bubbles between electrodes, in order to explain the existence of optimum condition. Furthermore, water electrolysis experiments were conducted using potassium hydroxide (KOH) aqueous solution and platinum (Pt) electrodes under atmospheric pressure, and rising velocity, bubble diameter and local current density were measured. These experimental data were obtained for estimating the present model.

Nomenclature

- d : bubble diameter, m
- E : cell voltage, V
- E_c : reversible potential + overvoltage other than ohmic loss by bubbles, V
- F : Faraday constant (= 9.65×10^4 C/mol)
- H : electrode height, m
- k : parameter defined by Eq. (11)
- P : system pressure, Pa
- R : universal gas constant (= 8.3143 J/mol·K)
- T : system temperature, °C or K
- u : bubble rising velocity, m/s
- W : width of electrode, m
- x : coordinate along electrodes, m

Greek symbols

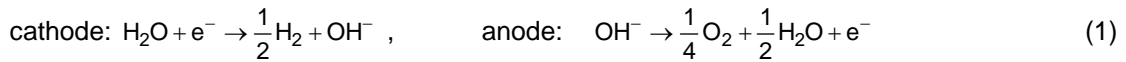
- α : mean void fraction between electrodes
- α_x : local void fraction
- α_{op} : mean void fraction at optimum condition
- δ : electrodes space, m
- δ_{min} : electrodes space at water electrolysis limit, m
- δ_{op} : electrodes space at optimum condition, m
- Φ : mean current density, A/m²
- Φ_x : local current density, A/m²
- ρ : specific resistance, Ω m

2. Model of Water Electrolysis

2-1. Outline of model

In this chapter, a model of alkaline water electrolysis is explained, considering the electrolysis cell configuration as shown in Fig.1. From both electrodes (cathode and anode), hydrogen and oxygen

bubbles are generated, respectively, subject to the following reaction formula when cell voltage is large enough.



Bubbles are considered to rise up between electrodes under gravitational field. Therefore, as vertical position, x , increases, local void fraction, α_x , gradually increases that causes the decrease of local current density, Φ_x , as shown in Fig.1.

In this model, the following situations were assumed:

- i) Cell voltage (electric potential difference) is independent of position, x ,
- ii) Bubble rising velocity, u , is constant in the whole area between electrodes, i.e. bubble rising velocity is uniform along vertical and horizontal directions,
- iii) The summation of reversible potential and overvoltage other than ohmic loss by bubbles is independent of current density, and
- iv) Diaphragm is omitted for simplicity.

In commercial water electrolyzers, diaphragm is indispensable for separating hydrogen gas from oxygen gas. This model, however, neglected the diaphragm since it aims mainly to show the existence of optimum condition due to bubbles between electrodes. For the next step, diaphragm should be included in advanced model where precise information on two phase flow and ions diffusions are considered.

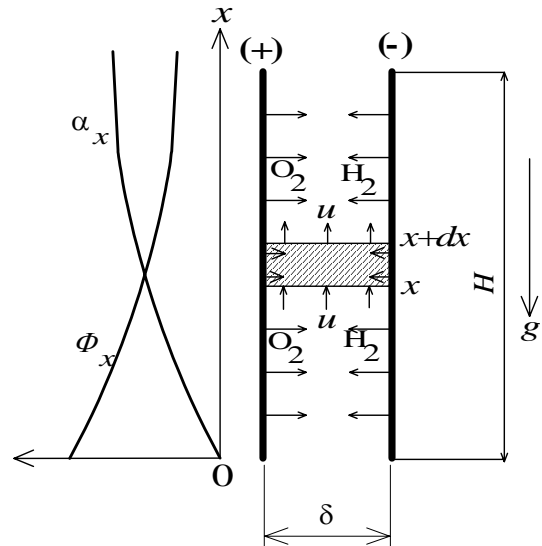


Fig.1 Electrolysis cell configuration in the model

2-2. Basic relations

Firstly, consider the balance of bubble volume at differential control volume, $\delta \cdot W \cdot dx$, as shown in Fig.1. Here, δ and W denote electrodes space and width of electrode, respectively. Since the mass fluxes of hydrogen and oxygen gas are proportional to local current density, the volume flux of hydrogen and oxygen gas generated from each electrode can be expressed as follows, assuming ideal gas law can be applied.

$$\text{cathode (H}_2\text{): } \frac{1}{2} \frac{RT}{P} \frac{\Phi_x W}{F} dx \quad [\text{m}^3/\text{s}] , \quad \text{anode (O}_2\text{): } \frac{1}{4} \frac{RT}{P} \frac{\Phi_x W}{F} dx \quad [\text{m}^3/\text{s}] \quad (2)$$

then,

$$\text{total (H}_2\text{+ O}_2\text{): } \frac{3}{4} \frac{RT}{P} \frac{\Phi_x W}{F} dx \quad [\text{m}^3/\text{s}] \quad (3)$$

where P : system pressure, R : universal gas constant, T : system temperature, and F : Faraday constant ($= 9.65 \times 10^4$ C/mol).

Therefore, by introducing local void fraction, α_x , and bubble rising velocity, u , the bubble volume balance at the control volume leads to the following equation.

$$\delta W u (\alpha_x + d\alpha_x) - \delta W u \alpha_x = \frac{3}{4} \frac{RT}{P} \frac{\Phi_x W}{F} dx \quad (4)$$

then,

$$\delta u \cdot d\alpha_x = \frac{3}{4} \frac{RT}{FP} \Phi_x \cdot dx \quad (5)$$

Equation (5) shows the relation among local void fraction, local current density and bubble rising velocity.

Secondly, Ohm's law is applied to the control volume. It is well known that electric resistance of electrolyte depends on void fraction, subject to several correlations (Kreysa and Kuhn, 1985). When Bruggemann's correlation is adopted, electric resistance at the control volume, dR_x , is estimated by

$$dR_x = \rho \frac{\delta}{W dx (1 - \alpha_x)^{3/2}} \quad (6)$$

where ρ is specific resistance of electrolyte.

Therefore, Ohm's law yields the following relation.

$$E - E_c = (\Phi_x \cdot W dx) \times dR_x = \Phi_x \cdot \frac{\rho \delta}{(1 - \alpha_x)^{3/2}} \quad (7)$$

then,

$$\Phi_x = \frac{E - E_c}{\rho \delta} (1 - \alpha_x)^{3/2} \quad (8)$$

where E is cell voltage and E_c is summation of reversible potential and overvoltage other than ohmic loss by bubbles. Equation (10) shows the relation among local void fraction, local current density and cell voltage.

2-3. Void fraction and current density profiles

From basic relations, Eq.(5) and (8), void fraction and current density profiles can be deduced. Substitution of Eq.(8) into Eq.(5) yields the following relation.

$$\frac{1}{(1 - \alpha_x)^{3/2}} d\alpha_x = \frac{3 RT(E - E_c)}{4 \rho FP \delta^2 u} dx \quad (9)$$

Solving the Eq.(9) under boundary condition of $\alpha_x=0$ at $x=0$, local void fraction profile can be obtained.

$$\alpha_x = 1 - \left(1 + \frac{k(E - E_c) x}{\delta^2 u H} \right)^{-2} \quad (10)$$

Here, H denotes electrode height and parameter k is defined as follows.

$$k = \frac{3RTH}{8\rho FP} \quad (11)$$

Substitution of Eq.(10) into Eq.(8) yields local current density profile.

$$\Phi_x = \frac{E - E_c}{\rho \delta} \left\{ 1 + \frac{k(E - E_c) x}{\delta^2 u H} \right\}^{-3} \quad (12)$$

From Eq.(10) and (12), mean void fraction, α , and mean current density, Φ , can be easily obtained.

$$\alpha = \frac{1}{H} \int_0^H \alpha_x dx = \frac{k(E - E_c)}{\delta^2 u + k(E - E_c)} \quad (13)$$

$$\Phi = \frac{1}{H} \int_0^H \Phi_x dx = \frac{\delta u}{2\rho k} \left\{ 1 - \left(\frac{\delta^2 u}{\delta^2 u + k(E - E_c)} \right)^2 \right\} \quad (14)$$

2-4. Water electrolysis limit and optimum condition

Transformation of Eq.(14) yields the following relation among macro parameters of E, k, Φ , δ and u.

$$E - E_c = \left\{ \left(1 - \frac{2\rho k \Phi}{\delta u} \right)^{-1/2} - 1 \right\} \frac{u}{k} \delta^2 \quad (15)$$

Here, the value inside the square root must be positive, which leads to the following relation.

$$\delta > \delta_{\min} = 2 \frac{\rho k \Phi}{u} = 0.75 \frac{RTH\Phi}{FPu} \quad (16)$$

This minimum value of electrode space, δ_{\min} , is considered to show the limit of water electrolysis, below which water electrolysis can not be conducted since void fraction between electrode becomes too large (close to 100 %) and electric resistance between electrodes reaches infinity.

The efficiency of water electrolysis, η , can be expressed as follows.

$$\eta = \frac{\Delta H \cdot I \cdot \frac{1}{2F}}{I \cdot E} = \frac{\Delta H}{2F \cdot E} \quad (17)$$

where I is total electric current and ΔH is standard enthalpy of formation of water electrolysis (= 285.84 kJ/mol). The denominator and the numerator of Eq.(17) denotes total power used for water electrolysis and generated enthalpy due to water electrolysis per unit time, respectively. It is easily understood from Eq.(17) that the efficiency of water electrolysis is inversely proportional to cell voltage. Therefore, the efficiency is discussed by cell voltage in this paper; i.e. higher efficiency is equivalent to smaller cell voltage at a certain electric current.

The optimum condition of water electrolysis where the efficiency, η , becomes maximum corresponds to the minimum cell voltage. Therefore, when mean current density, electrodes height, electrolyte concentration, system temperature and pressure are set constant, the optimum condition can be expressed by the following equation since E_c is also constant.

$$\frac{d(E - E_c)}{d\delta} = 0 \quad (18)$$

Then, from Eq.(15) and (18), we obtain the electrode space at the optimum condition, δ_{op} , as follows.

$$\delta_{op} = 3.390 \frac{\rho k \Phi}{u} = 1.271 \frac{RTH\Phi}{FPu} (= 1.695\delta_{min}) \quad (19)$$

The mean void fraction at the optimum condition, α_{op} , can be obtained from Eqs.(13), (15) and (19).

$$\alpha_{op} = 0.3596 \quad (20)$$

Equation (20) implies that the optimum condition is realized when mean void fraction is about 0.36.

2-5. Summaries of the model

The above model can show the following relations only if bubble rising velocity, u , is known.

- i) relation among macro parameter (E , Φ , δ , H , ρ , T , P): Eq.(15)
- ii) relation between water electrolysis efficiency, η , and cell voltage, E : Eq.(17)
- iii) profiles of local void fraction, α_x , and local current density, Φ_x : Eqs. (10) and (12)
- iv) as a derivative result, the optimum condition, δ_{op} and α_{op} : Eqs. (19) and (20)
- v) as a derivative result, the water electrolysis limit, δ_{min} : Eq.(16)

This model succeeds to clearly exhibit the existence of optimum condition, in addition to water electrolysis limit, considering the effects of bubbles between electrodes. For future works, diaphragm will be included in advanced model in order for simulating commercial electrolyzers correctly.

3. Experiments for Model Estimation

3-1. Outline of experiments

In this chapter, experiments for model verification are reported. Firstly, bubble rising velocity and bubble diameter distribution between electrodes were measured to evaluate model predictions explained in the last chapter. As stated before, bubble rising velocity is indispensable for model predictions. Bubble diameter distribution was measured since it is considered to have close relations with bubble rising velocity. In addition, the relations between cell voltage and electrodes space were measured to exhibit optimum condition. Secondly, current density profile was measured for verification of the model, using experimental results of bubble rising velocity.

3-2. Experimental setup for measurements of bubble rising velocity, bubble diameter and optimum condition

Figure 2 shows the outline of experimental setup for alkaline water electrolysis, mainly for measuring bubble rising velocity and diameter. The water electrolysis of potassium hydroxide (KOH) aqueous solution was conducted under atmospheric pressure using platinum (Pt) plates as electrodes. Inside the liquid container (280mm width x 150mm depth x 280mm height) made of vinyl chloride, the electrodes were completely immersed and fixed in parallel with a space designated to 1, 1.5, 2, 2.5, 3, 4, 5, 10 and 20 mm. The height of electrodes was set to 100mm. The width of electrodes was set to either 50 mm or 5 mm. DC power supplier enabled DC current up to 100A and DC voltage up to 35V

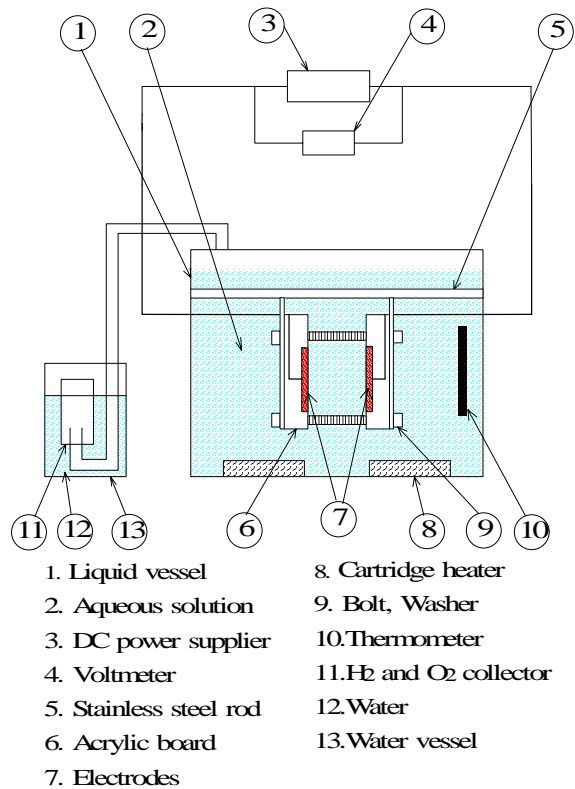


Fig.2 Outline of experimental setup

between electrodes: current density ranged from 0.1 to 1.6 A/cm² by 0.1 A/cm² step. Hydrogen and oxygen gases generated were collected to collector bottle through water. The temperature of the KOH aqueous solution was controlled to 20 and 40°C by cartridge heaters. The concentration of KOH aqueous solution was set to 8.5, 17.0 and 25.5wt%. The cell voltage and DC current were measured by voltmeter and ammeter, respectively.

Visual images of two phase flow between electrodes were obtained by a digital video camera (DVC) with 30 frames per second and a digital microscope. The video images of whole area between electrodes recorded by the DVC, as shown in Fig.3, were sent to a personal computer where the bubble rising velocity was measured by the following method: the movement of a group of bubbles was traced between several frames (the order of 0.1 s) and the distance of movement was measured by using a ruler set close to electrodes. The images of bubbles taken by the microscope, as shown in Fig.4, were sent to the personal computer, and bubble diameters were measured by using an image processing software.



Fig.3 Two phase flow pattern between electrodes
 ($\Phi=1.0\text{A/cm}^2$, $T=40^\circ\text{C}$, $C=40\%$)



Fig.4 Microscope image of H₂ bubbles

3-3. Experimental results of bubble rising velocity, bubble diameter and optimum condition

Figure 5 shows the relation between cell voltage and electrodes space with mean current density as a parameter when system temperature was 40°C, the concentration was 8.5% and electrode width was 50 mm, for an example. As reported before [10], there were optimum conditions of water electrolysis shown in Fig.5: i.e. the minimum cell voltage at a certain mean current density. The optimum space, δ_{op} , gradually increased from 1.5mm to 2.5mm as mean current density increased. This experimental result is in qualitatively good agreement with the model prediction of optimum space expressed by Eq.(19).

Figure 5 also shows the existence of water electrolysis limit, δ_{min} , as predicted by the model, Eq.(16), where the mean current density was rather large ($>1.2\text{ A/cm}^2$). At smaller electrodes space than δ_{min} , where

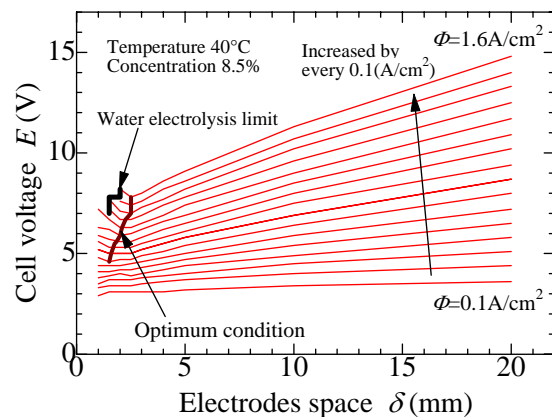


Fig.5 Relation between cell voltage and electrodes space
 (optimum condition and water electrolysis limit)

experimental data are not appeared in Fig.5, DC current supplier could not keep constant values of current and voltage since void fraction between electrodes are considered to fluctuate significantly at a very large value. The relation of Eq.(19), $\delta_{op} = 1.695\delta_{min}$, also seems reasonable judging from Fig.5.

Figure 6 shows the experimental results on bubble rising velocity, u , at electrodes space $\delta = 20\text{mm}$ for electrode width 50mm . As shown in Fig.4, bubble rising velocity was found to increase almost linearly as mean current density increased, ranging $4 \sim 24\text{cm/s}$. As the concentration became larger, bubble rising velocity decreased and its temperature dependence could not be neglected; i.e. as system temperature increased, bubble rising velocity increased. For smaller concentration, system temperature had little effects on bubble rising velocity at $\delta = 20\text{mm}$. As for reference, the mean void fraction at the experimental condition of Fig.6 ranged $1 \sim 9\%$, that could be estimated by bubble rising velocity and mean current density.

For wide electrodes ($W=50\text{mm}$), bubble rising velocity could not be measured near the optimum condition because of high void fraction between electrodes. Therefore, bubble rising velocity at $\delta=2\text{mm}$, that is near the optimum condition, was measured for narrow electrodes ($W=5\text{mm}$), as shown in Fig.7. Bubble rising velocity at $\delta=2\text{mm}$ becomes larger than that of $\delta=20\text{mm}$, since void fraction becomes larger at $\delta=2\text{mm}$. The bubble rising velocity measured at $\delta=2\text{mm}$ for $W=5\text{mm}$ will be used for model estimation later.

Figure 8 shows the relation between mean bubble diameter and mean current density. Bubble diameter increased almost linearly as mean current density increased. This relation is considered to have significant influences onto the increase of bubble rising velocity as shown in Fig.6.

Figures 9(a)~(c) illustrate the bubble diameter distribution at electrodes space $\delta = 20\text{mm}$, concentration $17\text{ wt}\%$ and system temperature 40°C . As mean current density increased from $\Phi=0.1\text{A/cm}^2$ to $\Phi=1.0\text{A/cm}^2$, bubble diameter distribution changed to the larger range, as stated at Fig.8. Figure 9 also shows that bubble diameter ranged from the order of 0.01mm to 0.4mm . The criterion of bubbles departure from electrodes seems unrevealed so far in the literatures, in addition that the mechanism of bubble coalescence has not been clearly modeled. Therefore, for the future work, the bubble departure criterion and the coalescence mechanism in water

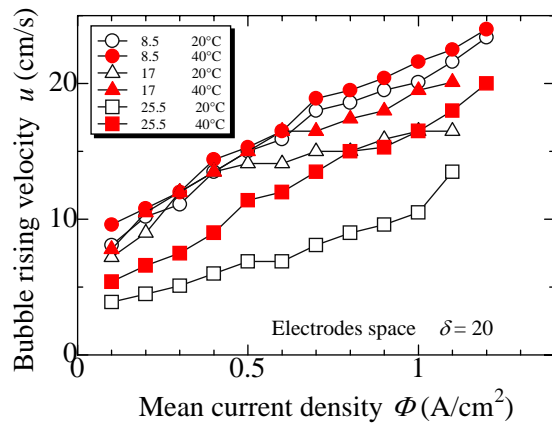


Fig.6 Relation between bubble rising velocity and mean current density ($\delta=20\text{mm}$, $W=50\text{mm}$)

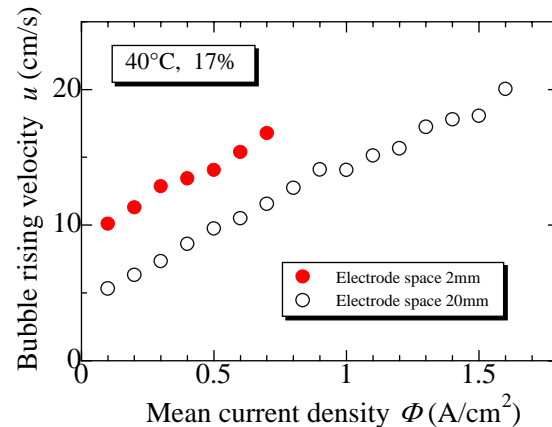


Fig.7 Relation between bubble rising velocity and mean current density ($W=5\text{mm}$)

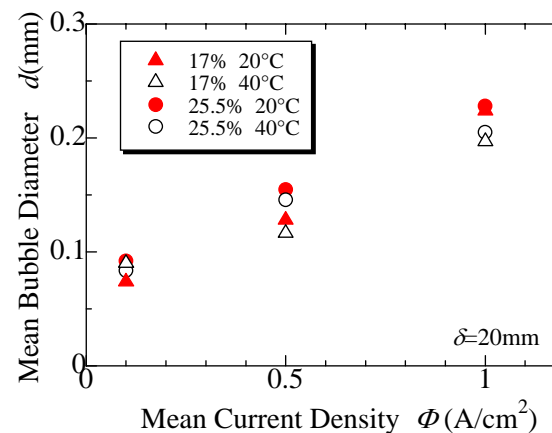


Fig.8 Relation between mean bubble diameter and mean current density ($\delta=20\text{mm}$)

electrolysis should be investigated experimentally and theoretically.

3-4. Model estimation of optimum condition and water electrolysis limit

The bubble rising velocity data measured at $\delta=2\text{mm}$, as shown in Fig.7, were used to estimate model predictions of optimum condition, δ_{op} , (Eq.(19)) and water electrolysis limit, δ_{min} (Eq.(16)). Figure 10 shows the comparison between experimental data and model predictions for both δ_{op} and δ_{min} . Model predictions can be plotted only for smaller current density, since bubble rising velocity could not be measured for larger current density in this experiment. Experimental data of δ_{op} and δ_{min} are only for larger current density. This is because electrodes space was set to 1.0, 1.5, 2.0, 2.5 mm, which means electrode space smaller than 1.0 mm could not be measured in this experiment. However, the extrapolations of model predictions are in good agreements with experimental data. This result indicates that the model presented in this paper has sound validity.

3-5. Measurement of current density profile

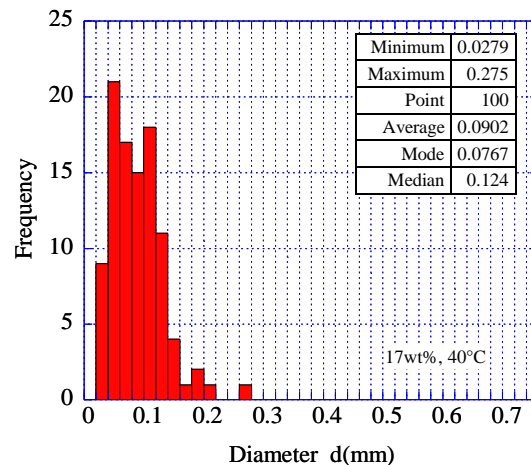
Local current density profiles were measured for another method of model verification. Experimental setup was almost the same with Fig.2 except the electrodes. To measure local current density, both electrodes were divided into 10 pieces (10mm height \times 50mm width each). Between each neighboring piece of electrodes, an insulating material of 1mm thickness was inserted, so that the total height of electrode became 109mm. The local current density of each piece of electrodes was measured while each cell voltage was kept as the same value. The experimental conditions were the same with those in the former experiments.

Figure 11 illustrates an example of comparison between experimental results and model predictions on local current density profile at $\delta=20\text{mm}$, concentration 8.5 wt% and system temperature 40°C. Model predictions were estimated from Eq.(12) by assuming the following conditions.

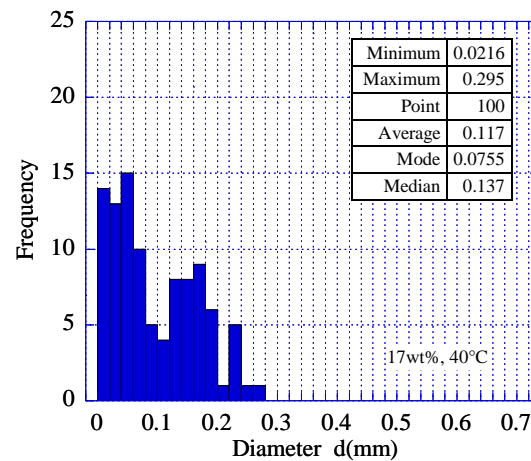
- i) Bubble rising velocity ($\delta=20\text{mm}$, concentration 8.5 wt% and system temperature 40°C) is a function of mean current density, correlated from Fig.6 and expressed as

$$u[\text{cm/s}] = 13.143\Phi[A/\text{cm}^2] + 8.5818 \quad (21)$$

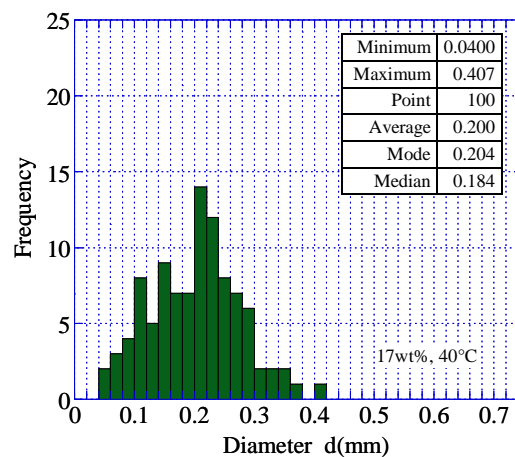
- ii) Constant component in cell voltage, E_c , that is summation of reversible potential and overvoltage other than ohmic loss by bubbles, is estimated as the cell voltage measured at $\delta=1\text{mm}$ and $\Phi=0.1\text{A/cm}^2$, where the effects of bubbles are considered to be negligible.



(a) $\Phi=0.1\text{ A/cm}^2$



(b) $\Phi=0.5\text{ A/cm}^2$



(c) $\Phi=1.0\text{ A/cm}^2$

Fig.9 Bubble diameter distribution
 ($\delta=20\text{mm}$, 17wt%, 40°C)

As seen from Fig.11, model predictions are in good agreement with experimental data except bottom and top areas of electrodes where bulk liquid may easily flow into regions between electrodes. Also for other experimental conditions, model predictions showed the same tendency with experimental results.

3-6. Summaries of experimental results

In spite that many assumptions were made as stated in the last chapter, measurement results of optimum conditions and local current density profile showed the sound validity of the present model utilizing the experimental results on bubble rising velocity.

4. Conclusions

A two phase flow model of alkaline water electrolysis was established, succeeding in explaining the influences of bubbles between electrodes on efficiency of alkaline water electrolysis, especially the existence of optimum condition and water electrolysis limit. For estimation of the model, optimum condition, bubble rising velocity, bubble diameter and local current density profile were measured, showing the sound validity of the model.

Acknowledgments

This research was supported by Grants-in-Aids for Scientific Research, Young Scientists (B), No.14750134, of Japan Society for the Promotion of Science.

References

- Abe, et al., Proc. 5th World Hydrogen Energy Conf., (1984), pp.727-736.
- Bongenaar-Schlenter, B.E., Janssen, L.J.J., Van Stralen, S.J.D. and Barendrecht, E., "The Effect of the Gas Void Distribution on the Ohmic Resistance during Water Electrolysis", J. Appl. Electrochem., Vol.15, (1985), pp.537-548.
- Funk, J.E. and Thorpe, J.F., "Void Fraction and Current Density Distributions in a Water Electrolysis Cell", J. Electrochem. Soc., Vol.116, (1969), pp.48-54.
- Hine, F. and Sugimoto, T., "Gas Void Fraction in Electrolytic Cell", Soda to Enso, (in Japanese), Vol.31, (1980), pp.347-362.
- Janssen, L.J.J. and Visser, G.J., "Distribution of Void Fraction, Ohmic Resistance and Current in a Tall Vertical Gas-Evolving Cell", Proc. Electrochem. Cell Des. Optim., Vol.123, (1991), pp.361-385.
- Kreysa, G. and Kuhn, M., J. Appl. Electrochem., Vol.15, (1985), pp.517-526.
- LeRoy, R.L., Janjua, M.B.I., Renaud, R., and Leuenberger, U., "Analysis of Time-Variation Effects in Water Electrolyzers", J. Electrochem. Soc., Vol.126, (1979), pp.1674-1682.
- Nagai, N., Takeuchi, M., Kimura, T. and Oka, T., "Existence of Optimum Space between Electrodes on Hydrogen Production by Water Electrolysis", Int. J. Hydrogen Energy, (2003), Vol.28, pp.35-41.

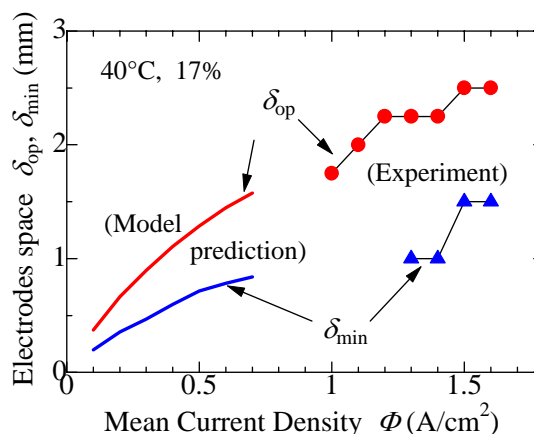


Fig.10 Comparison between model predictions and experimental data of δ_{op} and δ_{min}

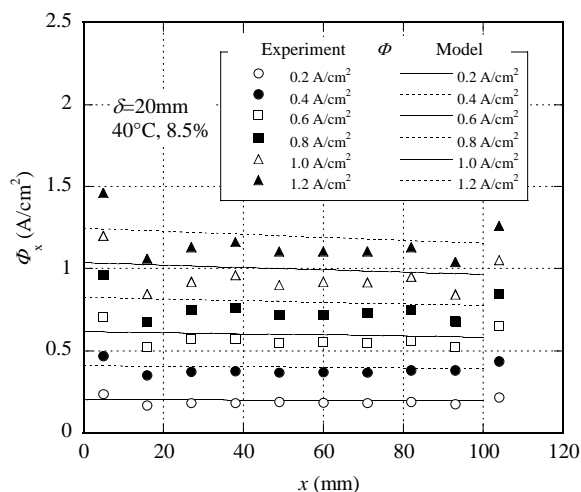


Fig.11 Local current density profile for comparison of model and experiment ($\delta=20\text{mm}$, 8.5wt%, 40°C)

- Riegel, H., Mitrovic, J. and Stephan, K., "Role of Mass Transfer on Hydrogen Evolution in Aqueous Media", *J. Appl. Electrochem.*, Vol.28, (1998), pp.10-17,.
- Sandstede, G. and Wurster, R., "Modern Aspects of Electrochemistry", edited by White, R.E. et al., No.27, Prenum Press, (1995), p.411.
- Winter, C.J. and Nitsch, J., "Hydrogen as an Energy Carrier – Technologies, Systems, Economy –", Springer-Verlag, 1988.